Model Features of a Cardiac Iontophoretic Drug Delivery Implant

Steven P. Schwendeman,[1,2] Vinod Labhasetwar,[1] and Robert J. Levy[1,3]

Received September 8, 1994; accepted December 20, 1994
KEY WORDS: iontophoresis; controlled release; ion exchange; cardiac arrhythmia; percolation; drug delivery implant.

INTRODUCTION

A new generation of implants has been reported over the last ten years that are capable of modulating the delivery of drugs following administration. These have included predominantly mechanical drug pumps (1), and the electromagnetic (2) and ultrasonic-based systems (3). In addition to these more conventional approaches, elegant self-regulated delivery systems have also been investigated (see Kost and Langer for review (4)). While the field of iontophoresis has been studied extensively for the transdermal route of drug administration (see reviews (5–6)), reports of the use of iontophoretic devices capable of being implanted for any significant duration of time (e.g., one month) are scarce or nonexistent.

We have used the basic principles of ion exchange, ion transport, and percolation to build theoretical models which describe iontophoretic transport of therapeutic cations through heterogeneous cation-exchange membranes (HCMs) composed of cation-exchange resin beads dispersed in silicone rubber (7–9); these membranes have been prepared and studied to develop the concept of implantable iontophoretic drug delivery. In this report we enter the next critical phase, which involves applying these theories and practical experience to design and fabricate an iontophoretic implant capable of long-term drug delivery.

General design criteria for membranes in an iontophoretic implant consist of rate-control, biocompatibility, durability against fracture, membrane permselectivity for the therapeutic ion (high transport efficiency leading to low power requirement), and time-responsiveness. In addition, some applications may require that the implant be flexible (e.g., cardiac implant attached directly to a beating heart). HCMs have been shown to fit five of the six above criteria (7–9). While the biocompatibility of sulfonated polystyrene beads in the HCMs is unknown, the silicone rubber matrix component is known to be biocompatible (10). Therefore, we have selected these membranes for incorporation into our cardiac-implantable iontophoretic device. For a material to form an inert reservoir to carry the drug solution, we have chosen pure silicone rubber, since silicone may be covalently attached directly to preformed HCMs during vulcanization (7), and this polymer possesses high mechanical strength, elasticity, and flexibility (10).

While implantable iontophoresis may have a number of important clinical applications (7–9), our present interest concerns a novel approach to therapy for patients with heart disease who experience recurrent cardiac arrhythmias (11). By delivering antiarrhythmic agents directly to the heart using drug-polymer implants, problems associated with conventional systemic delivery (e.g., drug toxicity and bioavailability limitations) have been shown to be reduced or eliminated (12–18). In addition, the onset of arrhythmias is often sudden, and a patient may not be able to receive treatment in time to prevent irreversible damage to the myocardium or death. Thus, the necessity for timely and localized delivery, taken together with the serious nature of heart disease, may require a sophisticated controlled-feedback drug delivery system such as an iontophoretic implant (in conjunction with an electrocardiogram monitoring system) to provide the best treatment (19).

This report discusses our general modeling approach for designing iontophoretic implants that incorporate heterogeneous cation-exchange membranes, describes both the pracical issues as well as how we have applied transport theory to design cardiac iontophoretic implants as a new method to deliver antiarrhythmic agents directly to the heart to treat cardiac arrhythmias, and finally, compares the *in vitro* delivery characteristics of an antiarrhythmic agent, sotalol, from these devices with that calculated from theory. These iontophoretic devices have been implanted epicardially in dogs for up to one month with highly efficacious results (20).

THEORETICAL SECTION

Development of Design Equations

The most useful design variable in preparing an iontophoretic implant is the maximum allowable leakage rate of drug from the device at zero current. For the case of membrane rate control (negligible boundary layer resistance), by integration of the steady-state Nernst-Planck equations (7), the rate of delivery for the drug cation (j_2A) from a donor reservoir filled with drug salt solution into a Na^+-containing medium during steady-state counter-diffusion is given as (subscript 1 = Na^+ and 2 = drug cation):

$$j_2A = \frac{\gamma \ln \gamma}{\gamma - 1} \frac{RT}{F^2 Rs_1} \qquad (off) \qquad (1)$$

where Rs_1 is the electrical resistance of the cation-exchange membrane in the presence of Na^+ and γ is the ratio of resistances of the membrane to transporting the two cations (Rs_1/Rs_2); R, T, and F are the gas constant, absolute temperature, and Faraday's constant, respectively. The above expression assumes an independence of counterion form of

[1] Department of Pediatrics and Communicable Diseases, and the College of Pharmacy, The University of Michigan, Ann Arbor, Michigan 48109-0576.
[2] Current Address: Department of Chemical Engineering, Massachusetts Institute of Technology, E25-342, Cambridge, Massachusetts 02139.
[3] To whom correspondence should be addressed.

0724-8741/95/0500-0790$07.50/0

the exchanger (i.e., swelling and accessibility to fixed charge sites not altered by the particular counterion).

For a specific drug, external salt concentration, and cation-exchanger, γ is fixed, as is the temperature of the body. Varying Rs_1 is the most convenient way to meet the zero current rate specification. Under the above conditions, this value will depend on membrane heterogeneity and geometry only. The heterogeneous component of HCM resistance was determined to obey a simple percolation scaling law (8). Although system size has not been thoroughly investigated, the resistivity was found to be constant for an appreciable range of membrane thickness for the size distribution of resin beads most studied (53 − 74 μm) (21). Thus, for this bead size combining equations (23) and (24) from ref (8) gives

$$Rs_1 = R_1^{ext}\left(\frac{\epsilon - \epsilon_c}{1 - \epsilon_c}\right)^{-2}\frac{L}{A} \tag{2}$$

where R_1^{ext} is the extrapolated resistivity of the resinous phase in the presence of Na^+ (HCM resistivity extrapolated to $\epsilon = 1$); ϵ and ϵ_c are the volume fraction of the resinous phase (membrane porosity) and the lower percolation threshold, respectively; L and A are the thickness and surface area of the membrane (wet ratio, L/A, is virtually equivalent to dry ratio). In addition, ϵ was related to the weight fraction of resin beads loaded into the membrane, l, via the swelling ratio of the membrane, SR, and SR was found to be linearly related to l ($SR = a + bl$). Thus, equation (26) from ref (8) to relate ϵ to l is given as

$$\epsilon = 1 + \frac{l - 1}{a + bl} \tag{3}$$

where a (dependent on bead loss from HCM) and b (dependent on resin water content) are constants. The above relationships were developed at a reference external salt concentration of 0.01 M, although cation-exchanger resistance is largely dependent on this variable. Since the Donnan exclusion of the cation-exchanger is virtually unaffected by increasing the salt concentration from 0.01 M to the physiologically relevant value (i.e., 0.15 M) (9), we may insert a factor that relates the resistances (or resistivity) of the membrane (or resin) at the two external salt concentrations as follows:

$$\alpha_c^{Ref} = \frac{Rs_1^{Ref}}{Rs_1^{c}} \tag{4}$$

where the superscripts "Ref" and "c" refer to reference (e.g., 0.01 M) and relevant (e.g., 0.15 M) salt concentrations of interest. Finally, while equation (1) has been shown to be highly accurate (e.g., <20% error) for ideal conditions (e.g., small drugs moving through large resin pores), a reproducible deviation from equation (1) is observed for larger drugs diffusing through modest pores at zero current (9). Therefore, we insert an appropriate correction factor in equation (1), $f_{(off)}^{nonideal}$, to account for this effect, which invalidates the independence of counterion form assumption. Hence, by combining equations (1)–(4) the *off* delivery rate is

$$j_2A = \frac{\gamma \ln \gamma}{\gamma - 1}\left[1 + \frac{l - 1}{a + bl}\frac{1}{1 - \epsilon_c}\right]^2 \alpha_c^{Ref} f_{(off)}^{nonideal}\frac{RT}{F^2 R_1^{ext,Ref}}\frac{A}{L} \qquad (off)$$

$$= \left[\begin{pmatrix} drug\ /\ Na^+ \\ resistance \\ factor \end{pmatrix}\begin{pmatrix} percolation \\ factor \end{pmatrix}\begin{pmatrix} external\ salt \\ concentration \\ factor \end{pmatrix}\begin{pmatrix} nonideal \\ factor \end{pmatrix}\begin{pmatrix} exchanger \\ constant\ (Na^+) \end{pmatrix}\begin{pmatrix} geometric \\ constant \end{pmatrix}\right] \tag{5}$$

and $R_1^{ext,Ref}$ is the extrapolated resin resistivity to Na^+ transport (the reference counterion) at a reference concentration of 0.01 M.

The other essential delivery rate for consideration is when the implant is turned *on* by applying a constant current. Under ideal transference conditions (no back-diffusion of counterions), this value may be determined directly from Faraday's law (22), since 100% of the charge moving across the membrane would be carried by the drug cation. However, typically this is only 70–90% accurate due to some co-ion transference (e.g., from Cl^-) between the resin and the silicone rubber. Therefore, we insert an appropriate correction factor in this instance ($f_{(on)}^{nonideal}$, equivalent to transference number) as follows:

$$j_2A = f_{(on)}^{nonideal}\frac{I}{F} \qquad (on) \tag{6}$$

where I is current.

Important for the development of a self-contained implant, which would require a battery as the power source, is the device potential (and device power requirement). Theoretical evaluation of this parameter is beyond the scope of this manuscript so we choose to evaluate simply the membrane potential (ϕ_m), while recognizing that ϕ_m will likely be the largest electric potential loss in the device. Since the boundary potential of the HCM will be small when separating solutions of similar salt concentration, ϕ_m may be evaluated from the resistance of the HCM to transfering the drug cation (Rs_2^c). In addition, the HCM (with Dowex 50W-2X) resistance in the presence of antiarrhythmics is known to be constant for an appreciable range of membrane potential (e.g., ~6 kΩ for 0.15 M acebutolol hydrochloride between 60-5000 mV from measurement in ref (9)). Thus, we may write from equations (2)–(4) with the receiver electrode as reference:

$$Rs_2^c = Rs_1^c\,\gamma^{-1} = \frac{1}{\gamma\alpha_c^{Ref}\left[1 + \frac{l - 1}{a + bl}\frac{1}{1 - \epsilon_c}\right]^2} R_1^{ext,Ref}\left(\frac{L}{A}\right) \tag{7}$$

and

$$\phi_m = Rs_2^c\, I \qquad (on) \tag{8}$$

To be certain that we do not exceed any limiting currents at the membrane and electrodes (i.e., the current where the normal processes required to maintain current flow such as diffusion in the unstirred boundary layers, crystallization of

AgCl, etc., reach their maximum output rate (24)), we consider the limiting diffusion current at the donor-side of the membrane corresponding to when the drug concentration is zero at this interface (the limiting current at the anode will be greater than the value at the membrane due to the larger surface area of the electrode). This subject is described in detail by Vetter (24) where in unstirred systems, a boundary layer is formed by natural convection (bulk flow due to sharp solution density gradient). Thus, we assume that at some limiting diffusion current there is a boundary layer in the donor-side of the membrane where the charge is transferred entirely by the drug cation ($j_2A = I/F$) and Cl^- is in electrochemical equilibrium (and thus, no net flux in boundary layer). This problem has been solved by integration of the steady-state Nernst-Planck equations of the two ions with boundary conditions consisting of the above flux constraint and concentration of the salt equal to the bulk salt concentration at the boundary layer thickness (24) of a verticle electrode plate:

$$I_{lim} = \frac{8}{3} F k \left[\frac{D_2^3 \alpha g}{\upsilon d}\right]^{1/4} C^{I\,5/4} A \qquad (9)$$

where the aqueous solution parameters, D_2, α, g, υ, and d, are the diffusion coefficient of the drug cation,[a] solvent density coefficient, acceleration due to gravity, solvent kinematic viscosity, and length scale (wet diameter) of the membrane, respectively; k is a constant (estimated values range between 0.51–0.73) relating the Nusselt number with the Prandtl and Grashof numbers, C^I is the donor salt concentration, and A is the wet surface area. Since the above expression is derived for an unstirred system, any mixing of the drug solution within the implant that might take place *in vivo* would reduce the boundary layer thickness and increase the above value. Thus, equation (9) represents the most conservative estimate of the limiting diffusion current within the device.

A final design variable that we consider is the response time (or lag time) required for the device to attain a steady delivery rate when turned *on* from the zero current state. Consistent with the assumptions described previously (8), the lag time from an initial case (c) $\Gamma_2 = \Gamma_2^{(off)}$, $\theta_L^{(c)}$, may be written as:

$$\theta_L^{(c)} = \frac{\left(\frac{m_{fc}^T}{\epsilon}\right)(\Gamma_2^{(on)} - \Gamma_2^{(off)})\,\Sigma}{\frac{I}{F}} \qquad (off \Rightarrow on) \qquad (10)$$

where Γ_2 is the fraction of the fixed charge sites in the transport path of the membrane that are occupied by the drug cation at steady-state; m_{fc}^T and Σ ($=[(\epsilon - \epsilon_c)/(1 - \epsilon_c)]^2$) are the total number of fixed charges in the membrane and the reduced membrane conductance, respectively.

The value of Γ_2 during a steady-state transference current (*on*) was determined from equation (18) from ref (8). Rearranging for the value of dimensionless current ($I^* = [(IF\mathrm{Rs}_1)/(RT)]$ with equations (2)–(4) gives

$$\Gamma_2^{(on)} = 1 - \frac{\gamma}{I^*} = 1 - \left[\frac{\gamma R T \alpha_c^{Ref}}{I F R_1^{ext,Ref}}\left(1 + \frac{l-1}{a+bl}\frac{1}{1-\epsilon_c}\right)^2\left(\frac{A}{L}\right)\right] \qquad (11)$$

Similarly, the value of Γ_2 during the *off* state may be determined by integrating the reduced drug concentration in the membrane (c_2*, determined from the integrated Nernst-Planck result, see (7)) over the entire membrane thickness noting that the value of reduced electric field (electric field normalized for $[RT/(FL)]$), s, is $(-\ln \gamma)$ at zero current, and from the expression for c_2^* ($=[(e^s - e^{s\xi})/(e^s - 1)]$):

$$\Gamma_2^{(off)} = \int_0^1 c_2^*(s,\xi)\,d\xi = \int_0^1 \frac{e^s - e^{s\xi}}{e^s - 1}\,d\xi = \frac{1}{1-\gamma} + \frac{1}{\ln \gamma} \qquad (12)$$

where ξ is the reduced position coordinate (normalized by L).

Thus, since m_{fc}^T ($= f_{SA}\, l\, W_m\, Q$) may be determined from the dry membrane weight (W_m), exchanger fixed charge capacity (Q, for Na^+ in dry form), fraction of HCM surface area exposed to the electrolyte (f_{SA}) and l, by combining equations (10)—(12), $\theta_L^{(c)}$ may be written as

$$\theta_L^{(c)} = \frac{l\left(1 + \frac{l-1}{a+bl}\frac{1}{1-\epsilon_c}\right)^2}{1 + \frac{l-1}{a+bl}} \times \left[1 - \left(\frac{\gamma R T \alpha_c^{Ref}}{I F R_1^{ext,Ref}}\right)\left(1 + \frac{l-1}{a+bl}\frac{1}{1-\epsilon_c}\right)^2\left(\frac{A}{L}\right) - \left(\frac{1}{1-\gamma} + \frac{1}{\ln \gamma}\right)\right](f_{SA} W_m)\frac{FQ}{I} \qquad (off \Rightarrow on) \qquad (13)$$

EXPERIMENTAL SECTION

Design of the Iontophoretic Cardiac Implant

The most basic requirements of an iontophoretic implant consist of a reservoir to hold the drug, a rate-limiting membrane, two electrodes, a source of electromotive force (e.g., a battery), a suitable biological interface if not the membrane above, and digital circuitry to control the current. Next, we must consider the potential for rate-limiting barriers between the HCM in the device and the extracellular fluid of the tissues that we are targeting. Levy et al. (12–13) have established the equivalence between *in vitro* and *in vivo*

[a] The diffusion coefficient in eq. (9) will actually be a function of the diffusion coefficients for both the drug cation and Cl^- as described by Agar (29), although for simplicity we have used the value of D_2, since it provides the most conservative (lowest) estimate for I_{lim}.

delivery rates of antiarrhythmic drugs (e.g., lidocaine and d-sotalol) from polymer matrices attached directly to the heart. This result indicates that there is no significant diffusion barrier for these compounds to enter the extracellular space of the epicardium at therapeutic dosing rates. Therefore, for acute evaluation of the implant, there is virtually no risk for additional rate-limits between the device and the highly perfused tissue. For chronic studies, we will have to consider the added effects of scar tissue to form around the implant (e.g., fibrous capsule formation). In addition, we have chosen to confine our current passage to within the device so that potential tissue damage or non pharmacological interference with the electrical rhythm of the heart may be avoided. Thus, by this rationale we have developed a configuration of a cardiac iontophoretic device described in Figure 1 (see below for method of fabrication).

For simplicity to illustrate our therapeutic concept, we have used an external galvanostat to supply the electrical current to the silicone rubber device. Two Ag/AgCl mesh electrodes for current passage are placed on either side of the HCM. The mesh is of high surface area to maintain low and uniform current density, which will prevent any limiting current at the electrodes (24). The device has two reservoirs: one large reservoir containing 0.15 M sotalol hydrochloride solution that delivers the drug to a second smaller passive reservoir. The second reservoir provides a medium for current passage and will allow the drug to diffuse freely through a biocompatible Millipore membrane (pore size 5 μm, Filter Type: SV, Millipore Inc., Bedford, MA) into the epicardium.

We formulated a HCM to passively deliver sotalol in this configuration at a rate that is suitably below previously established therapeutic delivery rates in dogs (~1 mg/h) (17). This was hypothesized to allow a ~20-fold increase in delivery rate when current is applied (900 μA) to exceed this therapeutic value. The input parameters of the formulation as well as the information necessary data to calculate design variables are listed in Table I.

Fabrication of the Implant

A cup-shaped silicone rubber reservoir with a 2 mL fluid capacity was prepared in a Teflon mold using Silastic Q7-4840 (supplied by Dow Corning, Midland, MI) and cured at 80°C for 2 hours (Figure 1). Ag/AgCl mesh electrodes (1.1 cm^2 (grid)/cm^2(actual), 0.72 cm^2 exposed surface area, Newark Wire Weaving Co., Hillside, NJ) were prepared by anodization in 0.6 N HCl. A circular disc of HCM (0.27 cm^2 of exposed area, 32 mg weight) was bonded to Silastic Q7-4840 by compression molding (80°C cure) so that the HCM formed a conducting port in the center of an insulated silicone membrane (7). The mesh electrodes were further bonded to the pure silicone portion of this membrane using Silastic Q7-4840 (80°C). This allowed the anode to be adjacent to the flat surface of the HCM. The cathode was formed with another Ag/AgCl mesh by attaching the electrode to the other side of the HCM, but separated by a silicone gasket spacer (compression molded Silastic Q7-4840). This HCM with attached electrodes was bonded to the reservoir with the anode inside and the cathode outside the reservoir using the Silastic as above. The cathode was further covered with a low protein binding, biocompatible Millipore membrane with a pore size of 5 μm (Filter Type: SV, Millipore Inc., Bedford, MA). The electrodes were connected to silicone rubber insulated pacing electrode leads to be connected to the constant current source.

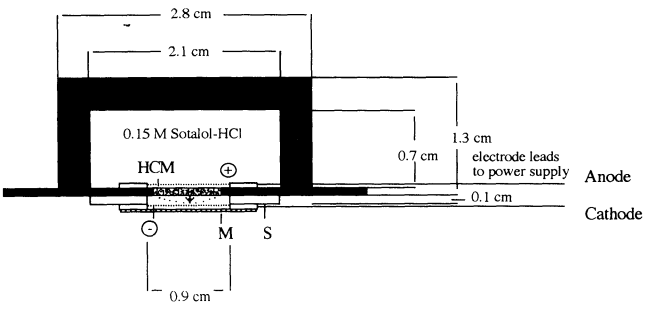

Figure 1. Schematic representation of a cardiac iontophoretic implant. The device consists of a silicone rubber reservoir filled with 0.15 M sotalol hydrochloride solution, a heterogeneous cation-exchange membrane (HCM), two Ag/AgCl electrodes, a silicone rubber spacer (S, between HCM and cathode(-)), and a 5 μm Millipore Membrane SV (M). The HCM swells outward toward the cathode(-) once in the presence of electrolyte.

Testing the Implant *in Vitro*

Following equilibration in 0.15 M NaCl solution for 2 days at 37°C, the device was filled with 2 mL of 0.15 M (d,l)-sotalol hydrochloride (Bristol Meyers Squibb, Wallingford, CT) by injecting through a 22 gauge syringe needle directly in the implant while simultaneously withdrawing the air with a second syringe. The HCM was converted from its original Na^+ form to sotalol form by placing the implant in a beaker containing the same sotalol solution, passing a current (150 μA) supplied from a galvanostat (University of Michigan Chemistry Shop, Ann Arbor, MI), and replacing the external solution until the device potential measured with a digital multimeter (Model 8062A, Fluke Mfg. Co, Everett, WA) had stabilized for some time. The implant was then stored in the off position while immersed in Sörensen buffer pH 7.3. For *in vitro* release, the implant was refilled with fresh 0.15 M sotalol hydrochloride solution and placed in a jacketed beaker containing 275 mL of Sörensen buffer at 37°C. The leads were then connected to a constant current source during on currents and the device potential was monitored across the leads with the digital multimeter. Two and one half off/on cycles were carried out for 1 h/1h time periods per cycle (20). Aliquots were taken without replacement and analyzed by ultraviolet spectrophotometry at 227 nm (The Perkin-Elmer Corp., Norwalk, CT) while maintaining perfect sink conditions.

RESULTS AND DISCUSSION

The steady-state *on* and *off* sotalol delivery rates were predicted to less than 12% error, indicating that the HCMs were responding properly (Figure 2); any significant defects in the device such as leaks would undoubtedly lead to large deviations of the observed delivery rates from those predicted, since any appreciable Cl^- transference would dramatically reduce the *on* delivery rate. The delivery rates were modulated ~20-fold over the current interval (0-900 μA), indicating the capability of the implants for modulating

Table I. Input Data and Constants for Calculation of Design Variables for the Cardiac Iontophoretic Implant

	Parameter	Value	Reference
Drug (sotalol) and	γ	0.079	(8)
Exchanger (Dowex 50W-2X)	Q	4.6 μmol/mg	(8)
Data	MW (hydrochloride)	309 g/mol	(26)
(Na^+ as reference counterion):	a	0.69	(8)
	b	3.5	(8)
HCM Percolation Data	ϵ_c	0.56	(8)
(Na^+ as reference counterion):	$R_1^{ext,Ref}$	3.5 kΩ-cm	(8)
HCM Geometric Parameters:[a]	l	0.42	
	L (dry)	620 μm	
	A (dry, wet)	0.27, 0.37 cm^2	
	d (wet)	0.69 cm	
	f_{SA}	(0.27/0.40)	
	W_m	32 mg	
Parameters in Aqueous Compartments:	C^I	0.15 M[a]	
	D_2	7.7×10^{-6} cm^2/s[b]	(27)
	α	0.059 L/mol[c]	(28)
	υ	0.70×10^{-2} cm^2/s[d]	(27,28)
Deviation from Reference and Ideality:	α_c^{Ref}	12	(9)
	$f_{(off)}^{nonideal}$	2	(9)
	$f_{(on)}^{nonideal}$	0.80	(9)

[a] Values in Materials and Methods.
[b] Determined from Hayduk-Laudie equation (27) using the additive method of Schroeder to calculate solute molal volume at the normal boiling point.
[c] Determined from density data as a function of concentration of NaCl interpolated to 37°C (28). Values of α to the 1/5 power are very weakly dependent on the particular univalent salt.
[d] Determined for pure water at 37°C from the quotient of viscosity (27) and density (28).

sotalol release. The lag time of the implants when turned on exhibited current dependence (2.1 ± 0.2, 6 ± 2, and 9.8 ± 0.4 min (mean ± sem, n = 3) for 900, 450, and 100 μA currents, respectively), although more modest than that predicted (4.7, 9.2, and 36 min for 900, 450, and 100 μA currents, respectively, from equation (13) and values in Table I). The theoretical lag time for the higher currents (450 and 900 μA) were quite close to experimental values and for the low current value (100 μA) more deviant. The latter result is likely due to the difficulty in attaining a true steady-state particularly under zero current conditions with the heterogeneous membranes, which contain fixed charge sites outside the highly conductive bead cluster (8). Since the HCMs were in sotalol form prior to the *off* phase (see *Experimental Section*), when the current is turned on, the above population of sites will predominantly contain sotalol and may cause a decrease in the observed lag time once the current is turn on. The lag times were produced by extrapolation of the linear portion of the non steady-state cumulative release curves (20).

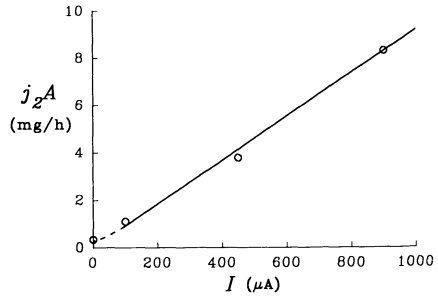

Figure 2. *In vitro* response of the iontophoretic device. The steady-state sotalol release rate (j_2A) is plotted versus the applied current (I). Symbols represent means (n = 6, or 10) during 2 ½ off/on cycles (20) and standard error bars were smaller than symbols. The solid line was calculated from equation (6) from values listed in Table 1. The dashed line arbitrarily connects *on* and *off* (0.30 mg/h from equation (5)) predictions.

The device potentials corresponding to the experiments described in Figure 2 were 0.9 ± 0.2, 5.0 ± 0.5, and 11.6 ± 0.4 V (mean ± sem, n = 4) for the 100, 450, and 900 μA input currents, respectively, indicating a device resistance of 9–13 kΩ. This is slighly greater than the calculated membrane resistance to sotalol transport of 5.7 kΩ from equation (7). Thus, other potential losses such as overpotential at the electrodes are likely contributing significantly to the device potential. Voltage losses due to concentration polarization (both within the boundary layers and at the interface) are not considered to contribute substantially to the device potential during transference. The calculated diffusion limiting current at the donor membrane boundary layer is 8400 μA from equation (9) by using k = 0.62. Thus, the concentration of salt will be depleted by ~10% at the surface of the membrane at the 900 μA, which will contribute only a neglible boundary layer and interfacial component (i.e., < 100 mV, (24)) to device potential. The high efficiency of drug delivery and device potential response at the highest applied current confirms that we have not exceeded this lim-

iting value, since large resistances accompanied by hydronium transference across the membrane would result (24).

Therapeutic dosing rates of (d,l)-sotalol by epicardial administration in dogs has been shown to be of the order ~1 mg/h (17). This implant is capable of delivering sotalol at rates 8-fold above and 3-fold below this value. The response time from the implant (off -> on) is on the order of minutes; it is important that this value be quite short, since there will be an additional lag time for the drug to reach the site of action by the local drug circulation. Finally the device potential when turned on is ~1 to 12 V at a power of ~1 to 10 mW. These values are within the capability of batteries developed for implantable pacemakers (25).

CONCLUSIONS

We have designed and fabricated a cardiac iontophoretic implant. Design equations describe the *on*/*off* rates, membrane component of device potential, and response time of the implant; these theoretical values, which are based on are previous modeling of a bi-ionic system (7–9), adequately described the transport behavior observed while testing the device *in vitro*. In addition, the *on* rates are in the region of therapeutic values previously established in dogs. The flexible device is prepared specifically for evaluating a new drug delivery system for the treatment of cardiac arrhythmias. Previous studies strongly suggest that this may be accomplished without passing a current through the cardiac tissue. Hence, these implants are determined to be suitable for examination in animals.

ACKNOWLEDGMENTS

Financial support to S.P.S. was provided by a Pharmaceutical Manufacturers' Association Foundation fellowship. This research was also supported by NIH Grant HL 41663 and an American Heart Association of Michigan Grant-in-Aid to V. L. and a National Heart Association Grant-in-Aid, 89-0654, to R.J.L. The authors wish to thank Dr. David Edwards for helpful discussions and his helpful review of this manuscript.

REFERENCES

1. K. T. Heruth. Medtronic synchromed drug administration system. *Ann. N. Y. Acad. Sci.* 531:72–75 (1988).
2. J. Kost, K. Leong, and R. Langer. Ultrasound-enhanced polymer degradation and release of incorporated substances. *Proc. Natl. Acad. Sci. U.S.A.* 86:7663–7666 (1989).
3. E. R. Edelman, L. Brown, J. Taylor, and R. Langer. *In vitro* and *in vivo* kinetics of regulated drug release from polymer matrices by oscillating magnetic fields. *J. Biomed. Mater Res.* 21:339–353 (1987).
4. J. Kost and R. Langer. Responsive polymeric delivery systems. *Adv. Drug. Del. Rev.* 6:19–50 (1991).
5. J. B. Phipps and J. A. Gyory. Transdermal ion migration. *Adv. Drug Del. Rev.* 9:137–176 (1992).
6. G. B. Kasting. Theoretical models for iontophoretic delivery. *Adv. Drug Del. Rev.* 9:177–199 (1992).
7. S. P. Schwendeman, G. L. Amidon, M. E. Meyerhoff, and R. J. Levy, Modulated drug release using iontophoresis through heterogeneous cation-exchange membranes: membrane preparation and influence of resin cross-linkage. *Macromolecules* 25:2531–2540 (1992).
8. S.P. Schwendeman, G. L. Amidon, V. Labhasetwar, and R. J. Levy, Modulated drug release using iontophoresis through heterogeneous cation-exchange membranes II: influence of cation-exchanger content on membrane resistance and characteristic times. *J. Pharm Sci.*, 83:1482–1494 (1994).
9. S. P. Schwendeman, G. L. Amidon, and R. J. Levy, Determinants of the modulated release of antiarrhythmic drugs by iontophoresis through polymer membranes. *Macromolecules* 26:2264–2272 (1993).
10. J. W. Boretos. Silicones. *Polym. Sci. Technol.* 8:87–98 (1975).
11. A. Waldo and A Wit. Mechanisms of cardiac arrhythmias. *The Lancet* 341:1189–1193 (1993).
12. A. Sintov, W. A. Scott, R. Siden, and R. J. Levy. Efficacy of epicardial controlled-release lidocaine for ventricular tachycardia induced by rapid ventricular pacing in dogs. *J. Cardiovasc. Pharmacol.* 16:812–817 (1990).
13. V. Labhasetwar, A. Kadish, T. Underwood, M. Sirinek, and R. J. Levy. The efficacy of controlled release d-sotalol-polyurethane epicardial implants for ventricular arrhythmias due to acute ischemia in dogs. *J. Controlled Release* 23:75–86 (1993).
14. A. Sintov, W. A. Scott, K. P. Gallagher, and R. J. Levy. Conversion of ouabain-induced ventricular tachycardia in dogs with epicardial lidocaine: pharmacodynamics and functional effects. *Pharm. Res.* 7:28–33 (1990).
15. A. Sintov., W. Scott, M. Dick, and R. J. Levy. Cardiac controlled release for arrhythmia therapy: lidocaine-polyurethane matrix studies. *J. Controlled Release* 8:157–168 (1988).
16. R. Siden, A. Kadish, W. Flowers, L. Kutas, B. K. Bieneman, J. DePietro, J. P. Jenkins, K. P. Gallagher, and R. J. Levy. Epicardial controlled-release verapamil prevents ventricular tachycardia episodes induced by acute ischemia in a canine model. *J. Cardiocasc. Pharmacol.* 19:798–809 (1992).
17. V. Labhasetwar, T. Underwood, M. Gallagher, G., Murphy, J. Langberg, and R. J. Levy, Sotalol controlled-release systems for arrhythmias: *in vitro* characterization, *in vivo* drug disposition, and electrophysiologic effects. *J. Pharm. Sci.*, 83:157–169 (1994).
18. V. Labhasetwar, T. Underwood, M. Gallagher, J. Langberg, and R. J. Levy. Epicardial controlled-release ibutilide: effects on defibrillation threshold and electrophyiologic parameters. *J. Cardiovasc. Pharmacol.* 24:826–840 (1994).
19. W. Chen, S. P. Schwendeman, V. Labhasetwar, and R. J. Levy. Techniques in cardiovascular drug delivery - surfactant derivatization, polymer implants, and iontophoresis, in *Polymeric Site-specific Pharmacotherapy*, A. J. Domb (ed.), John Wiley & Sons, N.Y., 1994, pp. 221–242.
20. V. Labhasetwar, T. Underwood, S. P. Schwendeman, and R. J. Levy. Iontophoresis for modulation of cardiac drug delivery. *Proc. Natl. Acad. Sci USA*, in press.
21. S. P. Schwendeman, R. J. Levy, H. A. Murphy, and G. L. Amidon. Influence of the silicone rubber matrix on the iontophoretc transport through heterogeneous cation-exchange membranes. *Pharm. Res.* 8:S–141 (1991).
22. J. O'M. Bockris and A. K. N. Reddy. *Modern Electrochemistry Vol I.*, Plenum Press, N.Y., 1970.
23. W. E. Morf. *The Principles of Ion-selective Electrodes and of Membrane Transport*, Elsevier Scientific Publishing Company, N.Y., 1981.
24. K. J. Vetter. *Electrochemical Kinetics*, Academic Press, N.Y., 1967.
25. H. G. Mond. Permanent cardiac pacemakers: techniques of implantation, testing and surveillance, in *Hurst's The Heart*, R. C. Schlant, R. W. Alexander, W. O'Rourke, R. Roberts, and E. H. Sonnenblick (eds.), McGraw Hill, Inc., N. Y., 1994, p. 823.
26. *The Merck Index*, 11th ed., Merck&Co., Inc., Rahway, NJ, 1982.
27. R. C. Reid, J. M. Prausnitz, and T. K. Sherwood. *The Properties of Gases and Liquids*, 3rd ed., McGraw Hill Book Company, N. Y., 1977.
28. *Perry's Chemical Engineers' Handbook*, 6th ed., R. H. Perry and D. Green (eds.), McGraw-Hill Book Company, N. Y., 1984, pp. 3–76, 3–83.
29. J. N. Agar. Diffusion and convection at electrodes. *Disc Faraday. Soc.*, 1:26–37 (1947).